FATIGUE OF WELDED ALUMINIUM T-JOINTS

T. Mann[1], B. W. Tveiten[2] and G. Härkegård[1]
[1] Norwegian University of Science and Technology, Trondheim, Norway,
torsten.mann@immtek.ntnu.no
[2] SINTEF Materials Technology, Trondheim, Norway

SUMMARY

The fatigue life of a welded aluminium T-joint made from beams with rectangular hollow section (RHS) has been predicted using a crack propagation analysis and compared with experimental results from joints with different residual stress levels. To include the effect of the residual stresses, the stress ratio was calculated locally and, via Walker's equation, introduced in the analysis. How to obtain Walkers exponent has been discussed in detail. The introduction of a local stress ratio provides good agreement between the experimentally and the analytically found S-N-curves. The effect of the residual stresses was successfully included in the analysis.

INTRODUCTION

Welded structures are known for their low fatigue strength, which mainly results from the existence of crack-like defects, high stress concentrations and tensile residual stress fields caused by thermal expansion. Aiming at an ever more efficient use of material and increased reliability, the fatigue behaviour of welds is a pivot point. Of course, welding may be replaced by some alternative joining method with higher fatigue strength, e.g. adhesive bonding [1]. This, however, is often neither possible nor wanted. In order to enhance the fatigue strength of welded joints, the weld may either be placed in a less stressed area or must undergo a post-welding treatment, e.g. shot peening or grinding. Shot peening introduces compressive residual stresses, whereas grinding reduces the stress concentration and removes welding defects. When compressive residual stresses at the weld toe are introduced, it is, of course, desirable to actively use their effect in design. This, however, can only be done if the residual stresses are known and their beneficial effect can be predicted. A possibility to achieve this is shown in this paper and the obtained results are compared with experimental data.

THEORY

Assessing the fatigue life of a welded component is complicated by large variations in weld geometry, welding defects, residual stresses and the question to which extent the fatigue life is covered by crack initiation and propagation. If no post-welding treatment to remove welding defects has been performed, it must be reasonable to assume a dominance of crack propagation and hence to assess the fatigue life using a crack propagation analysis. The assumption that crack propagation is the dominant part of the fatigue life is supported by the S-N-curve slope of approximately 3, given in various standards for welded structures.

The most frequently used model to describe fatigue-crack propagation is Paris' law,

$$\mathrm{d}a/\mathrm{d}N = C\Delta K^m \quad . \tag{1}$$

Applying Paris' law, starting at the threshold stress intensity factor range, ΔK_{th}, will underestimate life since $\mathrm{d}a/\mathrm{d}N$ near threshold is over-predicted. On the other hand, the real near threshold behaviour is difficult to assess and, if the cracks are short, they may even propagate below the long crack propagation threshold and this in addition at high rates. Near final fracture behaviour is not included in Paris' law and when using it, the number of cycles spent when approaching K_{Ic} is overestimated. However, the error made is very small, since the period near final fracture contributes only a small fraction to the total life.

Mean stress effect

The constant C in Paris' law depends on mean stress. To express this dependency, an equation suggested by Walker [2] may be used. He proposed an effective stress range at $R = 0$, $\Delta\sigma_{\text{Walker}}$, for crack propagation and fatigue failure of non-cracked structures as a function of maximum stress, $\sigma_{\max}$, and stress ratio, R. Expressed in terms of stress intensity factor range, Walker's equation can be written as

$$\Delta K_{\text{Walker}} = \Delta K \big/ \left(1 - R\right)^{1-\gamma} \quad . \tag{2}$$

One must distinguish between the Walker exponent, γ, for crack propagation and fatigue of a non-cracked component. In this paper γ denotes the Walker exponent for crack propagation. Walker's approach is not limited to positive stress ratios, however, extrapolating it to negative stress ratios may over-predict the effective stress intensity factor range, since some of the compressive part of a cycle would contribute to ΔK_{Walker}. Assuming that only the tensile part of a cycle, hence $K_{\max}$, contributes to crack propagation, the Walker exponent must be set to zero when $R < 0$.

Short cracks

Paris' law is strictly valid for the stable growth of long cracks only. To account for geometrically short cracks a concept involving the parameter a_0, often called the characteristic or intrinsic crack length, suggested by El Haddad et al. [3], may be used. Härkegård [4] generalized this approach by including the geometry function F which leads to

$$\Delta K = F \Delta\sigma \sqrt{\pi \left(a + a_0\right)} \quad . \tag{3}$$

The characteristic crack length, which marks the intersection between the behaviour of a structure containing a long crack and a non-cracked structure in the Kitagawa-Takahashi-diagram, is found from

$$a_0 = \Delta K_{\text{th}}^2 \big/ \left(F \Delta\sigma_{\text{D}} \sqrt{\pi}\right)^2 \quad , \tag{4}$$

where $\Delta\sigma_D$ is the fatigue limit. ΔK_{th} and $\Delta\sigma_D$ depend on mean stress. If the mean stress dependencies can be expressed with Walker's equation and $\gamma_D = \gamma_{th}$, a_0 is found to be independent of mean stress. However, in general $\gamma_D \neq \gamma_{th}$. It must be noted that extending the ΔK approach to short cracks is not straightforward, since the requirements for ΔK to be valid are not fulfilled.

A crack propagating at a weld toe

In general the geometry function, F, in Eq. 3 does not account for global and local stress concentrations resulting from attachment and weld toe radius, respectively. If, however, the initial crack is short enough, it will be subjected to these raised stresses and therefore propagate faster near the surface than the same crack in a plate. To include this effect a function M_k may be introduced, which is formally defined as the ratio of the stress intensity factor of a surface crack at the weld toe and the stress intensity factor of a the same surface crack in a plate. Bowness and Lee [5] derived a set of equations to calculate M_k for welded joints made from plates with a non load carrying weld, see Fig. 1.

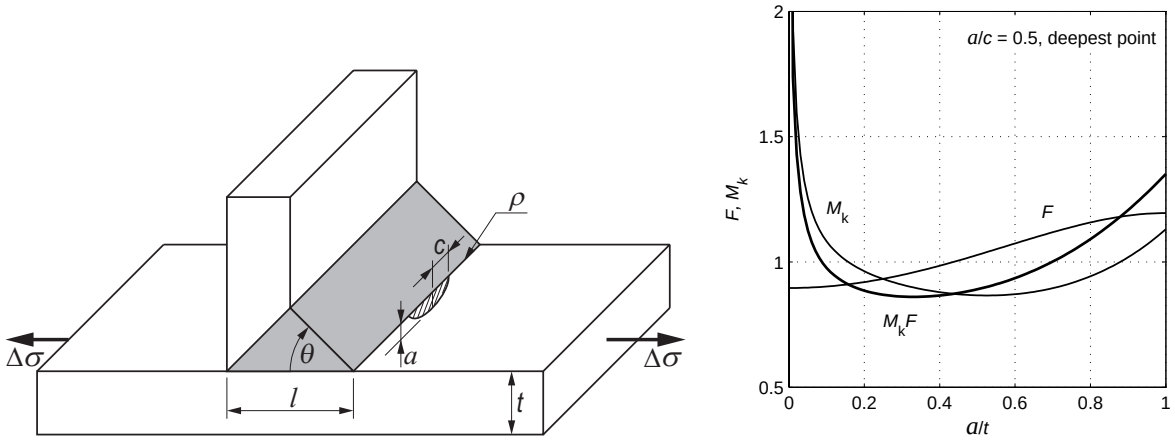

FIGURE 1.: (a) Geometry and variables used to derive M_k equation [5], (b) M_k ($\theta = 45°$, $l/t = 2$) for "as welded" weld toe radius [5] and F as functions of a/t.

EXPERIMENTAL RESULTS

T-joints, see Fig. 2a, produced from extruded 6082-T6 aluminium alloy rectangular hollow section profiles, were welded and tested at SINTEF Materials Technology, see Tveiten [6]. The profiles had a cross section of 40×60 mm with a wall thickness of 3 mm. The butt end of one tube was welded against the flat side of the other, see Fig. 2a, using fully automatic GMA-welding. Two series of specimens were tested. Welding the joints of the first series (batch 1), the profiles were simply kept in position, whereas in the joints of the second series (batch 2) a compressive residual stress field in loading direction at the weld toe was introduced. This was accomplished by elastically pre-straining the chord during the welding process. Examining the joints for initial cracks, none were found in the specimens of batch 1, whereas crack like defects with ≈ 0.1 mm depth were detected in some of the batch 2 specimens. Detecting initial cracks is, however, problematic, since they may be covered by cold flow at the weld toe..

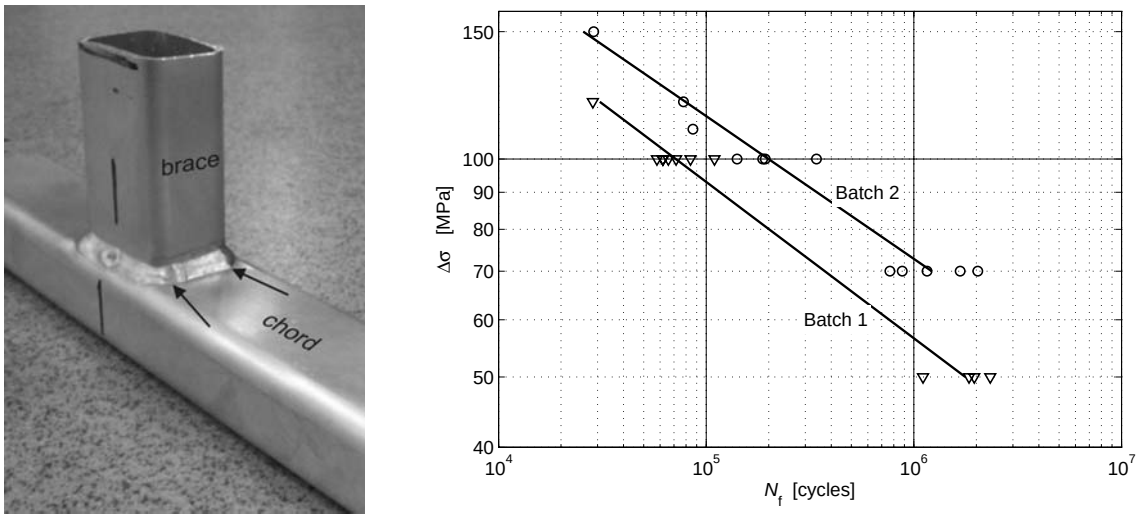

a) b)

FIGURE 2.: (a) Tested T-joints, (b) test results [6].

The specimens were subjected to 4-point bending at $R_{\text{nom}} = 0.1$. During testing it was found that cracks first become visible at one of the corners along the weld toe, see arrows in Fig. 2a. This behaviour could be expected, since the stress concentration is highest in those areas. Thereafter the crack propagates to a higher degree along the weld toe than a similar semi-elliptical crack in a plate, which is probably due to the high stress concentration and the existence of numerous crack-like defects along the weld toe. These defects grow independently at first and eventually coalesce to a large crack. Final fracture occurs almost immediately after the upper flange has fractured completely.

Using the least mean square method, Basquin's law,

$$N = A\Delta\sigma^{-m}, \tag{5}$$

was fitted to the test data. The obtained constants are given in Table 1.

TABLE 1: Basquin constants [6].

	m	A ($\Delta\sigma$ [MPa], N [cycles])
Batch 1	4.63	1.30×10^{14}
Batch 2	5.08	2.76×10^{15}

The standard deviation of $\log N$ is $s_1 = 0.11$ and $s_2 = 0.15$ for batch 1 and 2, respectively. The experiments showed that the fatigue life could be increased by approximately a factor 3 through the introduction of compressive residual stresses. Both, experimental results and the fitted curves are plotted in Fig. 2b.

PREDICTING THE FATIGUE LIFE OF WELDED RHS T-JOINTS

The crack growth approach outlined in the theory section is now applied to predict the fatigue life of the RHS T-joints described in the previous section. The material data used, are listed in Table 2. $R_{\text{p0.2}}$ and R_{m} are lower bounds received from Hydro Automotive. C, m and ΔK_{th} have been approximated from $\text{d}a/\text{d}N$ versus ΔK plots in Eurocode 9 [7].

TABLE 2: 6082-T6 aluminium alloy material data.

$R_{p0.2}$	R_m	m	$C\ \left(\mathrm{m/cycle},\ \mathrm{MPa}\sqrt{\mathrm{m}}\right)$		$\Delta K_{th}\ \left[\mathrm{MPa}\sqrt{\mathrm{m}}\right]$	$\Delta\sigma_D$ [MPa]
[MPa]	[MPa]		$R=0.1$	$R=0.8$	$R=0.1$	$R=0$
270	300	3.8	3.17×10^{-11}	6.34×10^{-11}	3	120

Local stress ratios to include residual stress

To predict the residual stresses, FE analyses using the program WELDSIM, were carried out [6]. However, those analyses were not detailed enough to give a residual stress distribution, but only a rough estimate, with numerical values given in Table 3. Using the relations between maximum, minimum and mean stress and stress range the stress ratio can be written as

$$R=\frac{\sigma_m-\Delta\sigma/2}{\sigma_m+\Delta\sigma/2}\ . \tag{6}$$

Local stress ratios, which include the residual stress, have been calculated from Eq. 6, where $\sigma_m=\sigma_{m,\,nom}+\sigma_{residual}$. "Local" is here only partly true, since the actual local stress field at the weld toe is not accounted for. Including the local stress distribution, however, makes only sense if the residual stress distribution is known as well. The local stress ratios for two stress ranges are given in Table 3. It can be seen that the actual stress ratio at the weld toe differs strongly from the nominal stress ratio and should therefore not be neglected when predicting fatigue life.

TABLE 3: Stress ranges, mean stresses, residual stresses and local stress ratios at the weld toe.

	R_{nom}	$\Delta\sigma$	$\sigma_{m,\,nom}$	$\sigma_{residual}$	σ_m	R
		[MPa]	[MPa]	[MPa]	[MPa]	
Batch 1	0.1	50	30.5	50	80.5	0.53
		100	61.1	50	111.1	0.38
Batch 2	0.1	70	42.8	-20	22.8	-0.21
		100	61.1	-20	41.1	-0.10

The Walker exponent

To account for the mean stress dependency with Walker's equation, the Walker exponent must be known. Walker [2] found $\gamma=0.5$ and $\gamma=0.425$ for 2024-T3 and 7075-T6, respectively, and Dowling [8] gives $\gamma=0.68$ and $\gamma=0.64$ for the same alloys. Since C is given at two different stress ratios, see Table 2, a Walker exponent can be calculated to $\gamma=0.88$. This seems rather high and using only two values is not a reliable method. In general, crack propagation data for 6000 series aluminium alloys is difficult to find. However, because of their frequent use in the aircraft industry, the data cover for 7000 series aluminium alloys, especially 7075-T6, is much better. Therefore, to estimate a more reliable Walker exponent, $\mathrm{d}a/\mathrm{d}N$ data have been extracted from [7-14] for the 7075-T6 aluminium alloy. The data points obtained are given in Fig. 3 in form of a ΔK versus R plot.

Distinguishing between different $\mathrm{d}a/\mathrm{d}N$ levels is required, since, due to the varying Paris exponents from the different sources, the Walker exponent will vary with $\mathrm{d}a/\mathrm{d}N$. Since the dependency of ΔK on R changes when R becomes negative, the Walker exponent will also change. Therefore, to obtain a continuous curve, the least mean square method must be modified. More precisely, two interpolation curves, one for $R \le 0$ and one for $R \ge 0$, must be found such that they intersect at $R = 0$. Taking the logarithm of Eq. 2 gives the linear relationship

$$y(x) = a + bx \ ,$$

(8)

with $y = \log \Delta K$, $x = \log(1-R)$, $a = \log \Delta K_{\mathrm{Walker}}$ and $b = 1 - \gamma$. Using the modified least mean square condition

$$\sum_i^n \left(y_i - y_1(x_i)\right)^2 + \sum_j^m \left(y_j - y_2(x_j)\right)^2 \overset{!}{=} \min \ ,$$

(9)

with $y_1(x) = a + bx$ and $y_2(x) = a + cx$, the two curves can be found. If the index i applies to data points at $R \le 0$, then j applies at $R \ge 0$. Partial differentiation with respect to a, b and c gives a system of linear equations to calculate a, b and c, and hence $\Delta K_{\mathrm{Walker}}$, $\gamma(R \le 0)$ and $\gamma(R \ge 0)$. Using the data points plotted in Fig. 3, the Walker exponents listed in Table 4 are obtained. The corresponding curves are plotted in Fig. 3. In addition the relation suggested by Elber [15] (for 2034-T3) has been included in Fig. 3.

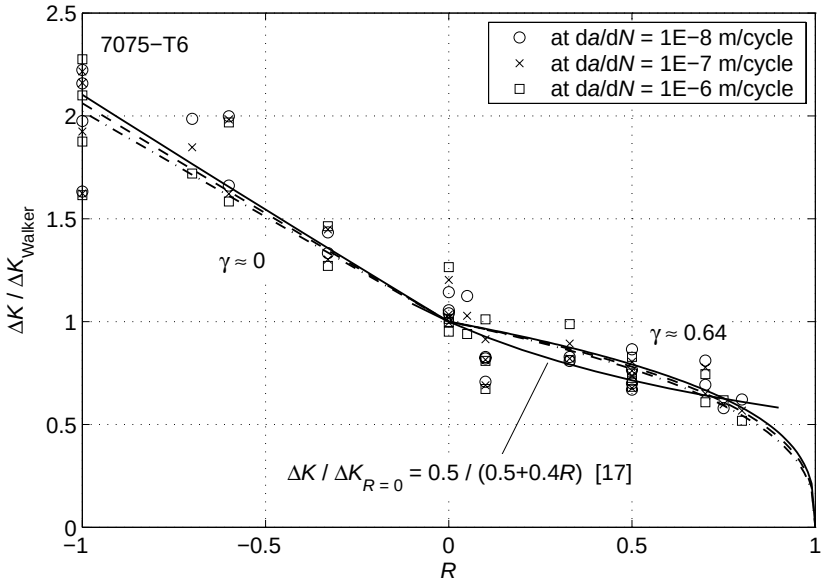

FIGURE 3: $\Delta K / \Delta K_{\mathrm{Walker}}$ as a function of stress ratio, R, for the crack propagation data obtained from [7-14] and the regression curves.

It is seen that, although the Paris exponents differ, the obtained Walker exponents are almost independent of $\mathrm{d}a/\mathrm{d}N$ and in good agreement with [8]. Based on the above Walker exponents and the fact that not enough data for the 6082-T6 aluminium alloy was available,

$\gamma = 0.5$ for $R \geq 0$ seems a reasonable choice. This has in addition the positive effect that a_0 is independent of R. For $R \leq 0$, $\gamma = 0$ was taken.

TABLE 4: Predicted Walker exponents for the 7075-T6 aluminium alloy.

$\mathrm{d}a/\mathrm{d}N$ [m/cycle]	$\gamma\ (R \leq 0)$	$\gamma\ (R \geq 0)$
1×10^{-8}	-0.07	0.66
1×10^{-7}	-0.04	0.64
1×10^{-6}	-0.02	0.62

Predicting the fatigue life

Assuming a propagating semi-elliptical surface crack, the fatigue life is found by integrating Eq. 1. Since the Paris constant C is given at $R = 0.1$ (and 0.8) and the applied local stress ratio differs from those values and, in addition, varies with $\Delta\sigma$, Walkers equation cannot be applied directly. At first C is transformed to $C(R = 0)$ using Eq. 2 and then, applying Eq. 2 again, $C(R = 0)$ adapted to the local stress ratio R. Inserting into Eq. 1, substituting ΔK and integrating, the total fatigue life can be expressed as:

$$N_\mathrm{f} = \frac{1}{C_\mathrm{l}}\left[\left(\frac{1-R_\mathrm{l}}{1-R}\right)^{1-\gamma}\Delta\sigma\sqrt{\pi}\right]^{-m}\int_{a_\mathrm{i}}^{a_\mathrm{f}}\left[F\,M_\mathrm{k}\sqrt{a+a_0}\right]^{-m}\mathrm{d}a\ . \tag{10}$$

The index 1 refers to the stress ratio at which the crack growth data are given and R without index is the local stress ratio. The initial crack depth, a_i, has been set to 0.05 mm, which is just below the resolution limit of the replica method used in [6] to find initial cracks. It must be mentioned that the predicted life is rather insensitive to the initial crack depth, which is because of the levelling effect of a_0. In addition, the stress peak at the surface gives a fast propagation. After examining the fracture surface, the final crack depth, a_f, has been set to 2.85 mm, which corresponds to 95 % of the sections wall thickness. Although the joint is subjected to 4-point bending, homogeneous tension can be assumed to prevail in the flanges, because of the thin walled-cross section. The geometry function, F, for a semi-elliptical crack in a plate, proposed by Newman and Raju [16], was employed. The equations to calculate F and M_k were developed for a plate and a joint made from plates, respectively. It is, therefore, not straightforward to apply them to hollow sections. The main problem is whether to set the "plate" thickness equal to the total section height or to the wall thickness. The geometry function F is relatively insensitive with respect to the thickness, see Fig. 1b, whereas M_k strongly depends on thickness. The larger the thickness the "deeper" is a crack "pushed" into the stress peak at the surface. It seemed, therefore, most realistic to use the wall thickness (3 mm) as "plate" thickness. The attachment footprint length l, see Fig 1a, was set to 6 mm, which approximately corresponds to the weld thickness. The initial crack aspect ratio was assumed to be $a/c = 0.5$. Equation 10 was numerically integrated using Simpson's rule. This was simultaneously done in a and c direction to allow the crack to reach the aspect ratio determined by F and M_k. Fig. 4 shows both, experimentally obtained S-N-curves and the predicted ones. Because of the varying local stress ratio, the predicted S-N-curves are no longer straight lines, but slightly curved. Experimental and predicted curve are

in good agreement for batch 2. The General agreement for batch 1 is also good, but the "slope" of the curves shows a significant difference, which becomes worse at lower stress ranges.

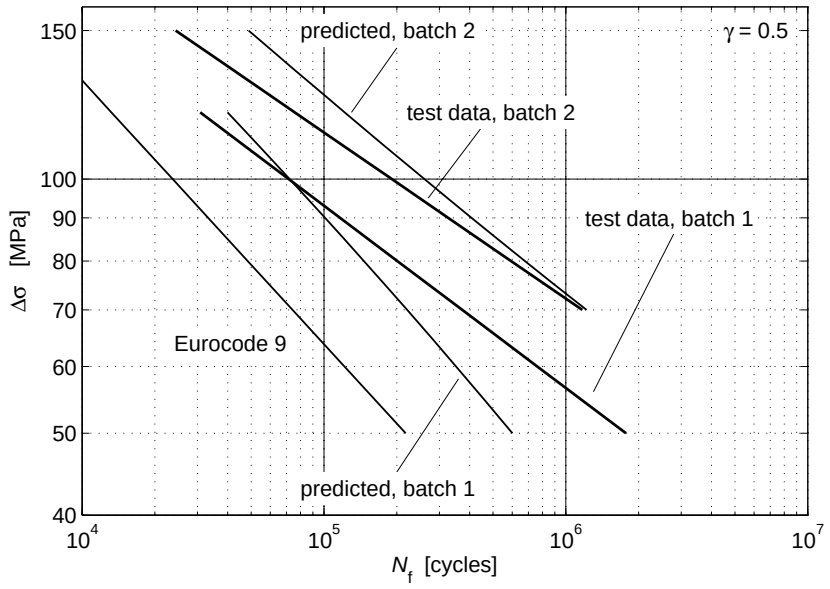

FIGURE 4: Predicted versus experimental S-N-curves.

CONCLUSIONS

The fatigue life of welded T-joints made from rectangular hollow sections has been calculated using a crack propagation analysis and compared with experimental results. The overall agreement is good. Still, the slopes of the S-N-curves differ in a way that suggests the existence of some crack initiation. The attempt to account for different residual stresses via local stress ratios and Walkers equation was successful. A Walker exponent derived directly for the 6082-T6 alloy and including the local and the residual stress distribution when calculating the local stress ratio may give even more realistic results.

REFERENCES

1. Sharp, M. L., Nordmark, G. E. and Menzemer, G. C., *Fatigue Design of Aluminium Components and Structures*. McGraw Hill, New York, 1996.
2. Walker, K., In *Effects of Environment and Complex Load History on Fatigue Life*, ASTM STP 462, Philadelphia, 1970, 1–14.
3. El Haddad, M. H., Smith, K. N. and Topper, T. H., *Journal of Engineering Materials Technology*, vol. **101**, 42–46, 1979.
4. Härkegård, G., In *Proceedings of the International Symposium of Fatigue Thresholds*, 867–879, Stockholm, 1981.
5. Bowness, D. and Lee, M. M. K., *International Journal of Fatigue*, vol. **22**, 369–387, 2000.
6. Tveiten, B. W., *The Fatigue Strength of RHS T-joints*. SINTEF report STF24 A03220, Trondheim, 2003.
7. Eurocode 9. *Design of aluminium structures – Part 2: Structures susceptible to fatigue*. European Prestandard ENV 1999-2, 1998.

8. Dowling, N. E., *Mechanical Behaviour of Materials*. Prentice Hall, London, 1999.

9. Bu, R. and Stephens, R. I., *Fatigue & Fracture of Engineering Materials & Structures*, vol. **9**, 35–48, 1986.

10. Hudson, C. M., *Effect of stress ratio on fatigue-crack growth in 7075-T6 and 2024-T3 Aluminum-alloy specimens*, NASA TN D-5390, Washington, 1969.

11. Durán, J. A. R., Castro, J. T. P. and Filho, J. C. P., *Fatigue & Fracture of Engineering Materials & Structures*, vol. **26**, 137–150, 2003.

12. Wu, X. R., Newman, J. C., Zhao, W., Swain, M. H., Ding, C. F. and Phillips, E. P., *Fatigue & Fracture of Engineering Materials & Structures*, vol. **21**, 1289–1306, 1998.

13. Fleck, W. G. and Anderson, R. B., In *Proceedings of the second International Conference on Fracture,* Brighton, edited by Pratt, P. L., Chapman & Hall, 1969.

14. *Damage Tolerant Design Handbook*. Metals and Cheramics Information Center, Battelle, 1972.

15. Elber, W., *Damage Tolerance in Aircraft structures*. ASTM STP 486, 230–242, 1971.

16. Newman Jr., J. C. and Raju, I. S., *Engineering Fracture Mechanics*, vol. **15**, 185–192, 1981.